Report No. R-102

Estimating Evaporation Using the Surface Energy Balance Model (SEBAL)

A Manual for NOAA-AVHRR in Pakistan

Yann Chemin
Mobin ud Din Ahmad

July 2000

International Water Management Institute,
Lahore, Pakistan

TABLE OF CONTENTS

1. INTRODUCTION

IWMI in Pakistan is completing an analysis on the assessment of water use performance in the Irrigated Indus Basin of Pakistan. In this regard, the amount of water used by the combination of vegetation and open soil evaporation has been calculated from the Surface Energy-Balance for Land model, SEBAL. A number of twenty images, spread over the two seasons Rabi 93-94 and Kharif 94, have been processed upon the Evaporative Fraction and daily Evaporation.

At present the SEBAL model processing used for the NOAA AVHRR images is explained and described under the Pakistan conditions. It is also brought to the reader's knowledge, practical difficulties undergone during the process, ranges of values for critical parameters and location of intermediate checking points.

This report is mainly to enable any person having Standard Remote Sensing Background to be able to achieve most of the processing of these Water Consumption parameters. Therefore, this manual is indicating steps to processing of NOAA AVHRR satellite imagery in order to get a basin wide data about land and water resources *on daily basis*. This means that on one hand it is not explicit on the theoretical justification of the equations used, the user of this manual, however, may refer to several publications cited at the end of the report. On the other hand, the *scale effect* for a so huge area has lead to modification, and other practical simplifications of the method, keeping the scientific accuracy nevertheless. Finally, each image is representative of *one single day*, leading the work on the time-scale of 24 hours which the reader has to bare in mind while using the set of interactive equations and spatial models.

2. VISIBLE REMOTE SENSING

2.1. Top of Atmosphere Reflectance

The main equation is:

$$\rho_i^{TOA} = \frac{L_i^{TOA}}{K_i} \qquad (-)$$

With:

ρ_i^{TOA} being the planetary spectral reflectance at the top of the atmosphere (-)

L_i^{TOA} the spectral radiance at the top of the atmosphere $\left(W.m^{-2}.\mu m^{-1}\right)$

K_i the incoming spectral radiance $\left(W.m^{-2}.\mu m^{-1}\right)$

$_i$ is the band number of the satellite (band 1 and 2)

In order to get to ρ_i^{TOA}, it is first to go to the two components of the ratio. Let us start with L_i^{TOA}, then finishing with K_i.

2.1.1. Spectral Radiance at the Top of the Atmosphere

$$L_i^{TOA} = \left(\frac{DN_i - I_i}{G_i}\right) \times \pi \qquad \left(W.m^{-2}.\mu m^{-1}\right)$$

With:

L_i^{TOA} the spectral radiance at the top of the atmosphere $\left(W.m^{-2}.\mu m^{-1}\right)$

G_i the gain (-) and I_i the offset $\left(W.m^{-2}.\mu m^{-1}\right)$

DN_i the Digital Numbers (-)

$_i$ is the band number of the satellite (band 1 and 2)

The gain and offset values for NOAA satellites are varying according to the NOAA satellite number, regarding the calculations, please refer to the Appendix A.

2.1.2. Drifts Correction of the Spectral Radiance

The gain and offset for band 1 and 2 are subject to drift. Calibration studies have shown that the sensor response drifts versus its own lifetime. The gain and the offset have to be corrected for this feature by the number of days between the launch (i.e. NOAA 14, December 12, 1994) and the date of acquisition. Bands 1 & 2 lie in the spectral range where reflectance is more pronounced than emittance. The spectral reflectance can be obtained after specifying the incoming radiance K_i

$$K_i = \frac{E_{oi}\cos\phi_{su}}{\pi d_s^2} \qquad \left(W.m^{-2}.\mu m^{-1}\right)$$

With:

K_i being the incoming radiance $\left(W.m^{-2}.\mu m^{-1}\right)$

E_{oi} the exo-atmospheric irradiance $\left(W.m^{-2}.\mu m^{-1}\right)$

Φ_{su} the Zenith angle *(rad)*

d_s Earth-Sun distance *(-)*

$_i$ is the band number of the satellite

Note on calculations of E_{oi}, ϕ_{su} and d_s

- E_{oi}, the exo-atmospheric irradiance $\left(W.m^{-2}.\mu m^{-1}\right)$ is fixed for NOAA satellites as following:

	NOAA 11	NOAA 14	Units
For band 1: E_{o1}	1629	1605	$\left(W.m^{-2}.\mu m^{-1}\right)$
For band 2: E_{o2}	1053	1029	$\left(W.m^{-2}.\mu m^{-1}\right)$

- ϕ_{su}, the Zenith angle *(rad)* is determined following this equation:

$$Cos\phi_{su} = \sin(\delta)\sin(latitude) + \cos(\delta)\cos(latitude)\cos(\omega) \qquad (rad)$$

With:

δ (rad) being the solar declination, the angular height of the sun above the astronomical equatorial plane. $\delta = 0.4093 \times \sin(\frac{2\pi}{365}J - 1.39)$ (rad), J being the Julian day number.

ω the solar angle hour varying following the time of the day. $\omega = \pi\left(\frac{t_{GMT} - 12}{12}\right)$ (rad), the time of the day t is in decimal hour, with t being: $t_{GMT} = t_{local} - long\left(\frac{24}{2\pi}\right)$

- d_s the distance Earth-Sun varying with the Julian day number *J*. $d_s = 1 + 0.01672 \times \sin\left(\frac{2\pi(J - 93.5)}{365}\right)$ (-), attention should be taken to calculate the sinus of the terms in parentheses in Radian mode, *not in Degree mode!*

2.2. ALBEDO CALCULATIONS

The calculation of the Albedo at the Earth surface involves two parts where first the single band surface reflectance is processed (i.e. Red and NIR bands) enabling the creation of the NDVI image, and in a second the step calculating the surface broadband Albedo from top of atmosphere reflectance.

2.2.1. Band-wise Albedo

Here has to be experienced the use of having a large area comprising of various type of geographical units. In the case of irrigation systems where often are large water bodies (dams, reservoirs, lakes…) and also very dry areas like desert, it is easy to set "tie-points" of steady surface reflectance. It has to be recalled at this stage that the scale factor is important while dealing with large area applications of Remote Sensing, therefore, the following system of "tie-points" is scientifically justified and correct.

The idea is to get the standard reference for surface reflectance values of extreme bodies like lakes and desert, that are to be fitted by a regression to the top of atmosphere reflectance values of the same places.

The following table is having the reference "tie-points" and their values in band 1 and 2 for the Pakistan study case:

Body	**long.**	**Lat.**	ρ_{0_1}	ρ_{0_2}
Water	67.6306	26.3994	0.0589	0.0348
Desert	69.4605	26.4552	0.3267	0.3436

The table below is showing the table to be filled by the operator from the top of atmosphere reflectance images, in order to fulfil the further steps i.e. the equation system solving.

Body	**long.**	**Lat.**	ρ_1^{TOA}	ρ_2^{TOA}
Water	67.6306	26.3994	ρ_{w1}^{TOA}	ρ_{w2}^{TOA}
Desert	69.4605	26.4552	ρ_{d1}^{TOA}	ρ_{d2}^{TOA}

In the case of Pakistan, the following set of equation solving has to be undergone:

Band 1	**Band 2**
$0.0589 = a_1 + \left(\rho_{w1}^{TOA}\right) \times b_1$	$0.0348 = a_2 + \left(\rho_{w2}^{TOA}\right) \times b_2$
$0.3267 = a_1 + \left(\rho_{d1}^{TOA}\right) \times b_1$	$0.3267 = a_2 + \left(\rho_{d2}^{TOA}\right) \times b_2$
Solving these equations lead to the following:	
$\rho_{0_1} = a_1 + \left(b_1 \times \rho_1^{TOA}\right)$	$\rho_{0_2} = a_2 + \left(b_2 \times \rho_2^{TOA}\right)$

With:

ρ_{0_i} the surface reflectance for band i. (-)

a_i and b_i the offset and the slope of the regression between ρ_{0_i} and ρ_i^{TOA} for band i. (-)

$\rho_{w_i}^{TOA}$ the top of atmosphere reflectance of water for band i. (-)

$\rho_{d_i}^{TOA}$ the top of atmosphere reflectance of desert for band i. (-)

2.2.2. Broadband Albedo

The broadband Albedo at the top of the atmosphere is required to get the surface one.

Therefore the following equation leads to the first step.

$$\rho^{TOA} = 0.035 + 0.545\rho_1^{TOA} + 0.32\rho_2^{TOA} \qquad (-)$$

With:

ρ^{TOA} being the top of atmosphere broadband Albedo (-)

ρ_i^{TOA} the top of atmosphere reflectance for band *i*. (-)

In order to get the broadband surface Albedo, expertise is required at this step, indeed it is to estimate the broadband path radiance (r_a) and the transmissivity of the atmosphere (τ_{sw}). How to determine them to input the following equation is explained in the Note below.

$$\rho_0 = \frac{\left(\rho^{TOA} - r_a\right)}{\tau_{sw}^2} \qquad (-)$$

With:

ρ_0 being the surface broadband Albedo (-)

ρ^{TOA} the top of atmosphere broadband Albedo (-)

r_a the broadband path radiance (-)

τ_{sw} the transmissivity single-way crossed by radiation of the atmosphere (-)

Note on broadband surface Albedo calculations

About the ranges of values for r_a and τ_{sw}, it should be stated that if the NOAA number for the image being processed is not known, or that previous stages were made with some doubts about coefficients; problems will arise at this stage. Indeed, ranges of data necessary to achieve the broadband Albedo test-point values will be extraordinary. These test areas are generally speaking, around 0.05 for the deep-water broadband Albedo and usually 0.35 for Rajasthan sand desert.

About tuning r_a and τ_{sw}, a definition of them

R_a	*The reflected part of the sun radiation on the top of the atmosphere*	from 0.02 up to 0.06
τ_{sw}	*The efficiency ratio of radiation conservation of the atmosphere between its top and the Earth skin surface.*	from 0.65 up to 0.85

The sun angle has a strong effect on r_a, being maximized at full reflection of sun on the top of the atmosphere. It can easily be assessed by a display of the NOAA image in 4/2/1 (normal color composition), showing a bright yellow zone covering some area of the image.

The vapor content and the dust particles in the atmosphere are generally responsible for lost of efficiency of the atmosphere to conserve the radiation circulating through it. In cloudy conditions, after removal of cloud, the surrounding areas (varying with the spatial distribution of the clouds and their nature) will be consequently full of water vapor. The case is the same in dry times where sandstorms are travelling from deserts up to areas of interest. In these conditions the τ_{sw} will be reduced accordingly to the density the operator is assessing.

2.3. NDVI Calculation

The surface NDVI calculation is taking the surface reflectance from the visible bands:

$$NDVI = \frac{\rho_{0_2} - \rho_{0_1}}{\rho_{0_2} + \rho_{0_1}} \qquad (-)$$

2.4. Surface Emissivity Calculation

Surface Emissivity estimated in the 8-14 μm range for sparse canopies

$$\varepsilon_0 = 1.009 + 0.047 Ln(NDVI) \qquad (-)$$

3. THERMAL REMOTE SENSING

Basically, the main output of the thermal remote sensing part is to have the surface temperature image. Different inputs are needed at this stage, some basic processing (correction and calibration of the thermal band) and the surface emissivity image (processed from NDVI).

3.1. Top of Atmosphere Corrections

Correction of band 4 drift

$$B_{TOA4} = -0.0167DN + 11.93 \qquad (W/m^2/Sr)$$

Black Body radiation at TOA for Band 4 (TIR_TOA4)

$$B_4(10.778, T) = B_{TOA4} \times \pi \times 0.92783 \qquad (W/m^2)$$

3.2. Meteorological Data and Spreadsheet Processing

In order to get the surface temperature, a number of steps have to be undertaken from meteorological data and some images products. The solving of the radiation emittance from the Earth will enable to calculate the surface temperature from the regression fitting with the spreadsheet data of temperature and the image data of the black body emittance at the top of the atmosphere.

3.2.1. Inputs Needed

From images:

- TIR_TOA4
- ε_0

From stations:

- Tmin air, Tmax air, Tavg air (= [Tmin air + Tmax air]/2)
- RH

3.2.2. Spreadsheet Processing

(1)	$E_{sat} = 6.11 \times e^{\left(\frac{17.27\times(T_{\max\_air}-273)}{T_{\max\_air}-273+237.3}\right)}$	(mbar)
(2)	$E_{act} = \left(\frac{RH \times E_{sat}}{100}\right)$	(mbar)
(3)	$\varepsilon_{atm} = 1.34 - 0.14\sqrt{E_{act}}$	(-)
(4)	$T_0 = T_{avg\_air}$ + Wim's table	(K)

(5)	$$B_0(\lambda, T_0) = \frac{C_1}{10.778^5 \times e^{\left(\left(\frac{C_2}{10.778 \times T_0}\right)-1\right)}}$$	$(W/m^2/\mu m)$
(6)	$\varepsilon_0 B_0(\lambda, T_0) = B_0(\lambda, T_0) \times 0.92783 \times \varepsilon_0$	(W/m^2)
(7)	$$B_{atm}(\lambda, T_{air}) = \frac{C_1}{10.778^5 \times e^{\left(\left(\frac{C_2}{10.778 \times T_{max\_air}}\right)-1\right)}}$$	$(W/m^2/\mu m)$
(8)	$\varepsilon_{tm} B_{atm}(\lambda, T_{air}) = B_{atm}(\lambda, T_{air}) \times 0.92783 \times \varepsilon_{atm}$	(W/m^2)
(9)	Total surf. Emittance = $\varepsilon_0 B_0(\lambda, T_0) + (1 - \varepsilon_0) \times \varepsilon_{atm} B_{atm}(\lambda, T_{air})$	(W/m^2)
(10)	$B_x(\lambda, T) =$ [Total surf. Emittance] a + b In-band radiation measured by NOAA at TOA (= TIR_TOA4) The regression helps to find a and b parameters: $a = \tau_{(\lambda)}$ in-band atmospheric transmittance *(-)* $b = L(\lambda, T_{TOA})$ in-band path radiance (W/m^2)	(W/m^2)
(10 bis)	Total surf. Emittance = $\frac{B_x(\lambda, T) - b}{a}$	(W/m^2)

The following table is the empirical relationship used in this study to relate Air temperature to soil's one.

T_{air}	T_0
10-15	+ 1
15-20	+ 3
20-25	+ 5
25-30	+ 7
30-35	+ 10
35 +	+ 13

Figure 1. Wim's Table.

3.3. SURFACE TEMPERATURE CALCULATION

(11)	$\varepsilon_0 B_0(\lambda, T_0) = \text{Total\_surf.\_emittance}$ $-\{(1-\varepsilon_0)\times[B_{atm}(\lambda, T_{air})\times\varepsilon_0 B_0(\lambda, T_0)\times 0.92783]$ Where the term inside [ ] is the average of grey-body radiation from atmosphere, from the equation 8.	(W/m^2)
(12)	$B_0(\lambda, T_0) = \dfrac{\varepsilon_0 B_0(\lambda, T_0)}{\varepsilon_0}$	$(W/m^2/\mu m)$
(13)	$T_0 = \dfrac{1.4388\times 10^4}{10.778\times Ln\left[\dfrac{0.92783\times 3.7427\times 10^8}{B_0(\lambda, T_0)\times 10.778^5}+1\right]}$	(K)

4. ENERGY BALANCE SOLVING

The energy Balance can be summarized at an instant *t* by the following equation:

$$Rn = G_0 + H_0 + \lambda E \qquad (W/m^2)$$

Where:

Rn	is the Net Radiation emitted from the Earth surface	*(W/m²)*
G_0	is the soil heat flux	*(W/m²)*
H_0	is the sensible heat flux	*(W/m²)*
λE	is the latent heat flux, being the energy necessary to vaporise water	*(W/m²)*

All the interest in solving the energy balance is to get the last component of it, the latent heat flux (λE), resulting in the following equation at an instant *t*:

$$\lambda E = Rn - G_0 - H_0$$

Therefore, each component will be calculated one by one in order to solve the system.

Remark: All inputs of this part, *unless specified*, are factors taken at *t* instantaneous time. Considering *t* the instantaneous time of the satellite overpass.

4.1. NET RADIATION

The net radiation is:

$$Rn = (1 - \rho_0) \times (K^{\downarrow}) + L^{\downarrow} - (\varepsilon_0 \sigma T_0^4) - (1 - \varepsilon_0) \times L^{\downarrow} \qquad (W/m^2)$$

with:

Rn	being the Net Radiation	*(W/m²)*
ρ_0	the surface reflectance	*(-)*
$K^{\downarrow}$	the solar radiation	*(W/m²)*
$L^{\downarrow}$	the averaged incoming broadband long-wave radiation of atmosphere from different meteorological stations (spreadsheet)	*(W/m²)*
ε_0	the surface emissivity	*(-)*
T_0	the surface temperature	*(K)*

4.1.1. Note on the Net Radiation Calculations

ρ_0, $K^{\downarrow}$, ε_0 and T_0 are all raster images data. Calculations of $K^{\downarrow}$ are dealt with in the next Note.

The incoming broadband long-wave radiation of atmosphere ($L^{\downarrow}$), is coming from the spreadsheet, where the Stefan-Boltzmann equation has to be applied for each meteorological station in order to be averaged for all station, giving $L^{\downarrow}$. Care should be taken in this regard to input the temperature values coming from the time being the closest to the instantaneous overpass time of the satellite. A minimum of two well-spread meteorological stations is nevertheless required to have sufficient accuracy. Five were used in this study, concentrated in the Indus Basin.

$$L^{\downarrow} = \sum_{i=2}^{i=n} \left[\varepsilon_{atm_i} \sigma T_{atm_i} \right] \qquad (W/m^2)$$

with:

$L^{\downarrow}$ the averaged incoming broadband long-wave radiation of atmosphere from different meteorological stations *(W/m²)*

ε_{atm_i} the atmospheric emissivity of the meteorological station i, already computed in the spreadsheet *(-)*

T_{atm_i} the atmospheric temperature at the meteorological station i already in the spreadsheet *(K)*

4.1.2. Note on the Instantaneous Solar Radiation Calculation

The solar radiation at t instantaneous time is:

$$K^{\downarrow} = \frac{K^{\downarrow}_{sun} \times \cos\phi_{sun} \times \tau_{sw}}{d_s^2} \qquad (W/m^2/\mu m)$$

with:

$K^{\downarrow}$	being the instantaneous solar radiation	*(W/m²/µm)*
$K^{\downarrow}_{sun}$	the sun external atmosphere radiation (constant = 1358)	*(W/m²)*
$\cos\phi_{sun}$	the cosinus of the sun zenith angle	*(rad)*
τ_{sw}	the atmosphere single-way transmissivity (determined by trial and error in the surface Albedo ρ_0 calculations, see 2.2.2)	*(-)*

4.2. Soil Heat Flux

The soil heat flux calculation is fairly simple; it is following the equation below:

$$G_0 = \frac{Rn - T_0}{\rho_0} \times \left(0.0032 r_0 + 0.0062 r_0^2\right) \times \left(1 - 0.978 \times NDVI^4\right) \qquad (W/m^2)$$

with:

Rn	being the Net Radiation	*(W/m²)*
T_0	the surface temperature	*(C)*
ρ_0	the surface reflectance	*(-)*
r_0	the day time average surface reflectance	*(-)*
NDVI	the Normal Difference Vegetation Index	*(-)*

4.2.1. Note on the Day Time Average Surface Reflectance R_0

To get r_0 while having the instantaneous surface Albedo (ρ_0), empirical relationship, valid only at large area is actually depending on the local time of overpass as shown below:

Local time of satellite overpass	ρ_0 to r_0 relationship
12.00	$\rho_0 = 0.9\ r_0$
14.00	$\rho_0 = r_0$
16.00	$\rho_0 = 1.1\ r_0$

4.3. Sensible Heat Flux

The sensible heat flux calculations are a set of iterations schematized in the following figure:

Iteration system for H calculations:

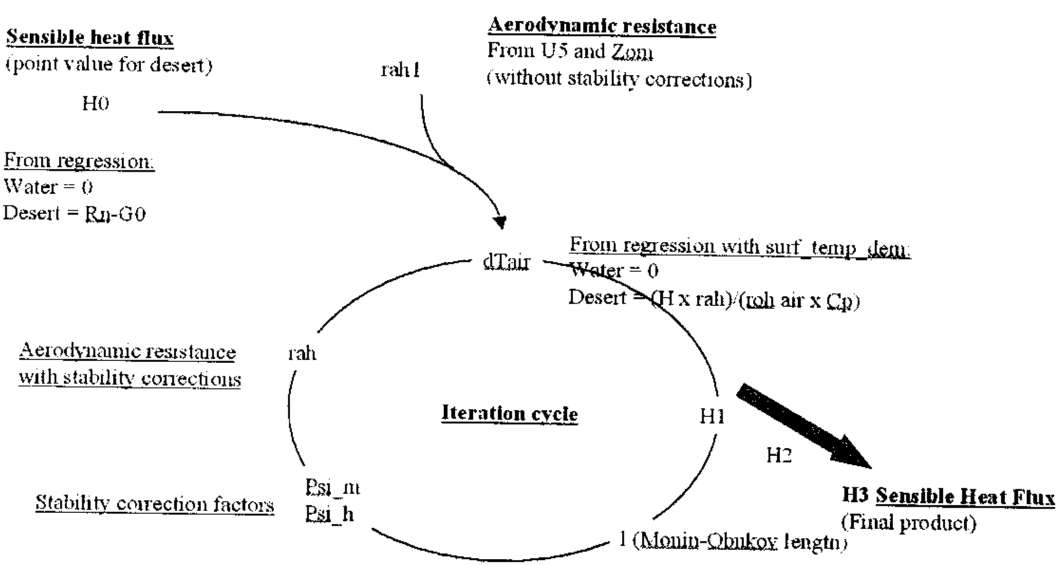

Figure 2. Summary of Sensible Heat flux calculations.

The whole interest of an iteration is to refine the value of a parameter, here it is the difference of Temperature between the Air and the soil surface. A good evaluation of this parameter is essential to assess the Sensible Heat Flux (H). One equation is the core of the cycle.

$$H = \frac{\rho_{air} \times C_p \times dT_{air}}{r_{ah}} \qquad (W/m^2)$$

With:

H	being the Sensible Heat Flux	(W/m^2)
ρ_{air}	the Atmospheric Air Density	(Kg/m^3)
C_p	the Air Specific Heat at Constant Pressure	$(J/Kg/K)$
dT_{air}	the Temperature difference between air (2 m) and soil surface	(K)
r_{ah}	the Aerodynamic Resistance to Heat transport	(s/m)

The iterations will focus on refining the image processing of the Sensible Heat Flux (H) by repeating the determination of the soil-air temperature difference (dTair) as a linear function of the DEM adjusted soil surface temperature *(T_0_dem)*. The variations arising in the dTair calculations are coming from the fact that r_{ah}, having psychometric buoyancy parameters for heat and momentum heat transfer can only be adjusted by iteration.

4.3.1. Calculation of the Starting dTair

From extreme situations the following arises:

For Desert: $dT_{air} = \dfrac{(R_n - G_0)\times r_{ah1}}{\rho_{air} \times C_p}$ with $H = R_n\text{-}G_0$

For Water: $dT_{air} = 0$

A linear relationship can be drawn out from these two values, linking T_0_*dem* and dT_{air}, giving the initial H image.

- A modified equation is used to calculate the first approximation of r_{ah1}, without correction from the psychometric parameters.

$$r_{ah1} = \frac{1}{U_5 \times 0.41^2} \times Ln\left(\frac{5}{z_{0m}}\right) \times Ln\left(\frac{5}{z_{0m} \times 0.1}\right) \qquad (s/m)$$

With:

r_{ah1}	the Aerodynamic Resistance to Heat transport (<u>first approximation</u>)	*(s/m)*
U_5	being the z = 5m wind velocity	*(m/s)*
z_{0m}	the aero-dynamical roughness length for momentum transport	*(m)*

<u>Raster images inputs:</u>

U_5 the z = 5m wind velocity
z_{0m} the aero-dynamical roughness length for momentum transport

- ρ_{air} the Atmospheric Air Density is responding to the added density of dry air and water vapor.

$$\rho_{air} = \left[\frac{P - \bar{e}_{act}}{T_0\_dem \times 2.87}\right] + \left[\frac{\bar{e}_{act}}{T_0\_dem \times 4.61}\right] \qquad (Kg/m^3)$$

With:

ρ_{air}	the atmospheric air density	*(Kg/m^3)*
P	the atmospheric air pressure	*(mbar)*
$\bar{e}_{act}$	mean actual water vapor pressure (from spreadsheet in 3.2.2)	*(mbar)*
T_0_*dem*	the surface temperature adjusted with the DEM	*(K)*

<u>Raster images inputs:</u>
T_0_*dem* the surface temperature adjusted with the DEM (T_0.dem = T_0 x 0.06 z)

- C_p is the Air specific Heat at constant pressure, C_p = 1004 J/Kg/K

From these, the Desert value of dT_{air} is calculated, making it possible to calculate the first Sensible Heat flux image (referred as H_1 in Figure 2) from the linear relationship of dT_{air} with T_0_dem completed with the water and desert values of dT_{air}.

4.3.2. Calculation of the First H approximation

This first iteration of the sensible heat flux (H_1) is the application of the main equation cited in the beginning of this section (4.3) with the above-mentioned calculated events. The equation will look this way:

$$H_1 = \frac{\rho_{air} \times C_p \times \left[a_1 + \left(b_1 \times T_{0-}dem\right)\right]}{r_{ah1}} \qquad (W/m^2)$$

With:

H_1	being the Sensible Heat Flux (<u>first approximation</u>)	(W/m^2)
ρ_{air}	the Atmospheric Air Density	(Kg/m^3)
C_p	the Air Specific Heat at Constant Pressure	$(J/Kg/K)$
T_0_dem	the surface temperature adjusted with the DEM	(K)
r_{ah1}	the first Aerodynamic Resistance to Heat transport approximation without corrections from psychometric parameters	(s/m)

<u>Raster images inputs:</u>

ρ_{air}	the Atmospheric Air Density
r_{ah1}	the Aerodynamic Resistance to Heat transport (<u>second approximation</u>)
T_0_dem	the surface temperature adjusted with the DEM

4.3.3. Calculation of the First Monin-Obukov Length

L_1 is computed from H_1, and is used into the next step, the psychometric parameters (φ_h and φ_m).

$$L_1 = \frac{\rho_{air} \times C_p \times \left(U_{*eff}\right)^3 \times T_{0-}dem}{K \times g \times H_1} \qquad (m)$$

With:

L_1	the Monin-Obukov Length (<u>first approximation</u>)	(m)
ρ_{air}	the Atmospheric Air Density	(Kg/m^3)
C_p	the Air Specific Heat at Constant Pressure	$(J/Kg/K)$
U_{*eff}	the effective friction velocity	(m/s)
T_0_dem	the surface temperature adjusted with the DEM	(K)
K	the Von Karman's Constant (0.4)	(-)
g	the gravitational force's acceleration (9.81)	(m/s^2)
H_1	being the Sensible Heat Flux (<u>first approximation</u>)	(W/m^2)

Raster images inputs:

ρ_{air} the Atmospheric Air Density
T_0_dem the surface temperature adjusted with the DEM
H_1 the Sensible Heat Flux (first approximation)

4.3.4. Calculation of r_{ah2} and the Psychometric Parameters

The parameters of interests are φ_h and φ_m. They are appearing in the r_{ah2} calculations in the following form:

$$r_{ah2} = \frac{1}{U_5 \times 0.41^2} \times Ln\left(\frac{5}{z_{0m}} - \varphi_{m1}\right) \times Ln\left(\frac{5}{z_{0m} \times 0.1} - \varphi_{h1}\right) \qquad (s/m)$$

With:

- r_{ah2} the Aerodynamic Resistance to Heat transport (second approximation) *(s/m)*
- U_5 being the z = 5m wind velocity *(m/s)*
- Z_{0m} the aero-dynamical roughness length for momentum transport *(m)*
- φ_{h1} the stability correction for the atmospheric heat transport (first approximation) *(-)*
- φ_{m1} the stability correction for the atmospheric momentum transport (first approximation) *(-)*

Raster images inputs:

r_{ah2} the Aerodynamic Resistance to Heat transport (second approximation)
U_5 the z = 5m wind velocity
T_0_dem the surface temperature adjusted with the DEM

The parameters φ_h and φ_m are defined as follow:

$$\varphi_{h1} = 2 \times Ln\left[\frac{(1+x_1)^2}{2}\right] \qquad (-)$$

$$\varphi_{m1} = 2 \times Ln\left[\frac{(1+x_1)}{2}\right] + Ln\left[\frac{(1+x_1)^2}{2}\right] - 2 \times A\tan(x_1) + \frac{\pi}{2} \qquad (-)$$

With $x_1 = \left[(1-16) \times \left(\frac{5}{L_1}\right)^{0.25}\right]$

- φ_{h1} the stability correction for the atmospheric heat transport (first approximation) *(-)*
- φ_{m1} the stability correction for the atmospheric momentum transport (first approximation) *(-)*
- L_1 the Monin-Obukov Length (first approximation) *(m)*

Raster images inputs:
L_1 the Monin-Obukov Length (first approximation)

4.3.5. Calculation of the Second dTair

From extreme situations the following arises:

For Desert: $dT_{air2} = \dfrac{H_1 \times r_{ah2}}{\rho_{air} \times C_p}$

For Water: $dT_{air2} = 0$

A linear relationship can be drawn out from these two values, linking T_0_dem and dT_{air2}, giving the second H image approximation.

4.3.6. Calculation of the Second H approximation

The calculation of the second H is dependent on the first equation of 4.3, where, this time, the components are:

Raster images inputs:

ρ_{air} the Atmospheric Air Density

r_{ah2} the Aerodynamic Resistance to Heat transport (second approximation)

T_0_dem the surface temperature adjusted with the DEM

$$H_2 = \frac{\rho_{air} \times C_p \times \left[a_2 + \left(b_2 \times T_0\_dem\right)\right]}{r_{ah2}} \qquad (W/m^2)$$

With:

H_2	being the Sensible Heat Flux (second approximation)	(W/m^2)
ρ_{air}	the Atmospheric Air Density	(Kg/m^3)
C_p	the Air Specific Heat at Constant Pressure	$(J/Kg/K)$
T_0_dem	the surface temperature adjusted with the DEM	(K)
r_{ah2}	the Aerodynamic Resistance to Heat transport with corrections from psychometric parameters (second approximation)	(s/m)

4.3.7. Calculation of r_{ah3}

L_2 the Monin-Obukov Length (second and last approximation) calculated from H_2, T_0_dem and ρ_{air}. This is enabling the calculation of φ_{h2} and φ_{m2}, psychometric parameters (second and last approximation).

r_{ah3} is then defined as:

$$r_{ah3} = \frac{1}{U_5 \times 0.41^2} \times Ln\left(\frac{5}{z_{0m}} - \varphi_{m2}\right) \times Ln\left(\frac{5}{z_{0m} \times 0.1} - \varphi_{h2}\right) \qquad (s/m)$$

With:

r_{ah3}	the Aerodynamic Resistance to Heat transport (third and last approximation)	*(s/m)*
U_5	being the z = 5m wind velocity	*(m/s)*
Z_{0m}	the aero-dynamical roughness length for momentum transport	*(m)*
φ_{h2}	the stability correction for the atmospheric heat transport (second and last approximation)	*(-)*
φ_{m2}	the stability correction for the atmospheric momentum transport (second and last approximation)	*(-)*

Raster input:

U_5 being the z = 5m wind velocity

z_{0m} the aero-dynamical roughness length for momentum transport

4.3.8. Calculation of the Third dTair

From extreme situations the following arises:

For Desert: $dT_{air3} = \dfrac{H_2 \times r_{ah3}}{\rho_{air} \times C_p}$

For Water: $dT_{air3} = 0$

A linear relationship can be drawn out from these two values, linking T_0_dem and dT_{air3}, giving the third (and last) H image approximation.

4.3.9. Calculation of H_3

The calculation of the third and last H is dependent on these components:

$$H_3 = \frac{\rho_{air} \times C_p \times \left[a_3 + \left(b_3 \times T_{0}\_dem\right)\right]}{r_{ah3}} \qquad (W/m^2)$$

With:

H_3	being the Sensible Heat Flux (third and last approximation)	*(W/m²)*
ρ_{air}	the Atmospheric Air Density	*(Kg/m³)*
C_p	the Air Specific Heat at Constant Pressure	*(J/Kg/K)*
T_0_dem	the surface temperature adjusted with the DEM	*(K)*
r_{ah3}	the Aerodynamic Resistance to Heat transport with corrections from psychometric parameters (third and last approximation)	*(s/m)*

Raster images inputs:

ρ_{air} the Atmospheric Air Density

r_{ah3} the Aerodynamic Resistance to Heat transport (third and last approximation)

T_0_dem the surface temperature adjusted with the DEM

5. 24 HOURS ENERGY BALANCE INTEGRATION

5.1. Net Radiation for 24 Hours

When calculating for the 24 hours net radiation, a different procedure is implemented than to get the instantaneous net radiation. This has an important meaning, for two different ways have to lead to the two terms (Rn_{24}, Λ) needed to get the actual ET on a 24 hours basis. This to avoid accuracy as well as a methodological concern that may arise on the validity of the ET actual 24 calculation from terms issued from the same sources.

The 24 hours net radiation is:

$$Rn_{24} = (1-\rho_0)\times(K_{24}^{\downarrow}) + L_{24}^{\downarrow} - (\varepsilon_0 B_{24}^{\uparrow}) - (1-\varepsilon_0)\times L_{24}^{\downarrow} \qquad (W/m^2)$$

with:

Rn_{24}	being the 24 hours Net Radiation	(W/m^2)
ρ_0	the surface reflectance	$(-)$
$K_{24}^{\downarrow}$	the 24 hours integrated solar radiation	$(W/m^2/\ m)$
$L_{24}^{\downarrow}$	the 24 hours averaged incoming broadband long-wave radiation of atmosphere from different meteorological stations (spreadsheet)	(W/m^2)
ε_0	the surface emissivity	$(-)$
$B_{24}^{\uparrow}$	the black body radiation from averaged daily air temperatures	(W/m^2)

5.1.1. Note on the 24 Hours Net Radiation Calculations

ρ_0, $K_{24}^{\downarrow}$, ε_0 and T_0 are all raster images data. Calculations of $K_{24}^{\downarrow}$ are dealt with in the next Note.

The outgoing black body radiation from atmosphere ($B_{24}^{\uparrow}$), is coming from the spreadsheet, where the Stefan-Boltzmann equation has to be applied with the averaged temperatures for all the stations.

$$B_{24}^{\uparrow} = \sigma T_{air24}^{4} \qquad (W/m^2)$$

with:

T_{air24}	the averaged daily temperature from several well spread meteorological stations	(K)
σ	the Stefan-Boltzman constant (5.67×10^{-8})	$(W/m^2/K^4)$

The incoming broadband long-wave radiation of atmosphere ($L_{24}^{\downarrow}$), is coming from the spreadsheet, where the Stefan-Boltzmann equation has to be applied with the daily average temperature for each meteorological station in order to be averaged for all station, giving $L_{24}^{\downarrow}$. A minimum of two well-spread meteorological stations is nevertheless required to have sufficient accuracy. Nevertheless, five were used in this study.

$$L_{24}^{\downarrow} = \sum_{i=2}^{i=n} \left[\varepsilon_{atm_i} \sigma T_{avgatm_i} \right] \qquad (W/m^2)$$

with:

$L_{24}^{\downarrow}$	the averaged incoming broadband long-wave radiation of atmosphere from different meteorological stations	*(W/m²)*
ε_{atm_i}	the atmospheric emissivity of the meteorological station i, already computed in the spreadsheet	*(-)*
T_{avgatm_i}	the daily average atmospheric temperature at the meteorological station i in the spreadsheet	*(K)*

5.1.2. Note on the 24 Hours Solar Radiation Calculation

The solar radiation at t instantaneous time is:

$$K_{24}^{\downarrow} = \frac{K_{sun}^{\downarrow} \times \cos\phi_{sun} \times \tau_{sw}}{\pi \times d_s^2} \qquad (W/m^2)$$

with:

$K_{24}^{\downarrow}$	being the average solar radiation on 24 hours	*(W/m²)*
$K_{sun}^{\downarrow}$	the sun external atmosphere radiation (constant = 1358)	*(W/m²/µm)*
$\cos\phi_{sun}$	the cosinus of the sun zenith angle	*(rad)*
τ_{sw}	the atmosphere single-way transmissivity (estimated constant for the day at 0.7)	*(-)*
d_s	the sun earth distance	*(A.U.)*

5.1.3. Note on Converting the 24 Hours Net Radiation into 24 Hours ET Potential

$$ET_{pot_{24}} = \frac{Rn_{24}}{L \times \rho_w} \times 86400.10^3 \qquad (mm/day)$$

With:

$ET_{pot_{24}}$	being the 24 hours potential evapotranspiration	*(mm/day)*
Rn_{24}	the net radiation on 24 hours	*(W/m²)*
L	the latent heat of vaporization	*(J/Kg)*
ρ_w	the density of fresh water	*(Kg/m³)*

- Where L can be calculated from the temperature image, providing the temperature input in Celsius degree:

$$L = [2.501 - (0.002361 \times T)] \times 10^6 \qquad (J/Kg)$$

With:

L	the latent heat of vaporization	*(J/Kg)*
T	the surface skin temperature	*(C)*

- Where ρ_w, the density of fresh water is 1000 Kg/m^3, however, in the case of Pakistan, considering the high concentration of material in the water, 1010 Kg/m^3 has been used.

5.2. Actual Evaporation for 24 Hours

The final part of this exercise is to calculate the actual evaporation for 24 hours by multiplying the ET potential on 24 hours by the evaporative fraction.

$$ET_{act24} = ET_{pot_{24}} \times \Lambda \qquad (mm/day)$$

with:

$ET_{pot_{24}}$ being the 24 hours potential evapotranspiration *(mm/day)*

Λ the evaporative fraction *(-)*

6. SUMMARY

Raster images needed for other raster images building

		OUTPUT Raster															
		NDVI	ρ_0	ε_0	T_0	$K^{\downarrow}$	Rn	G_0	Zom	U_5	ρ_{air}	rah	H_0	Λ	$K_{24}^{\downarrow}$	Rn24	$Etact_{24}$
INPUT Raster	NDVI			✓				✓	✓								
	ρ_0						✓	✓								✓	
	ε_0				✓		✓									✓	
	T_0						✓	✓			✓		✓				
	$K^{\downarrow}$						✓										
	Rn							✓						✓			
	G_0													✓			
	Zom									✓		✓					
	U_5											✓					
	ρ_{air}												✓				
	Rah												✓				
	H_0													✓			
	Λ																✓
	$K_{24}^{\downarrow}$															✓	
	Rn24																
	$Etact_{24}$																✓

7. APPENDIX A: NOAA CALIBRATION

The gain and offset for NOAA satellites are following the set of equation:

$$G_i = a_i t + b_i$$
$$I_i = c_i t + d_i$$

With:

t being the number of days after launch of NOAA

i the band number (band 1 and 2)

a_i, b_i, c_i, d_i coefficient varying with t and the band number

After Kerdiles (95?), coefficients a, b, c and d for the calculation of NOAA-11 and NOAA-14 AVHRR calibration coefficients (gain and offset) of channels 1 and 2[1]. The coefficients given for date D (line n) are valid up to the next date (line n+1). In other words these a, b, c and d coefficients must not be interpolated with time.

NOAA-11 Channel 1.

Date	Day post launch	a	b	c	d
24/09/88	0	-2.333e-04	1.704	1.220e-04	39.98
01/01/89	99	-3.079e-05	1.684	5.815e-05	39.99
01/01/90	464	5.412e-05	1.646	-4.236e-05	40.04
01/01/91	829	1.300e-06	1.689	-1.429e-04	40.12
01/01/92	1194	2.010e-05	1.666	-2.435e-04	40.24
01/01/93	1560	2.783e-05	1.654	3.832e-04	39.26
01/01/94	1925	-5.601e-05	1.815	0.000e-00	40.00
01/01/95	2290	-5.534e-05	1.814	0.000e-00	40.00

NOAA-11 Channel 2.

Date	Day post launch	a	b	c	d
24/09/88	0	-9.578e-04	2.606	1.623e-04	39.97
01/01/89	99	-3.049e-05	2.542	4.929e-05	39.99
01/01/90	464	9.108e-05	2.358	-1.284e-05	40.07
01/01/91	829	4.419e-06	2.397	-3.062e-04	40.20
01/01/92	1194	3.288e-05	2.410	-4.842e-04	40.43
01/01/93	1560	-4.630e-05	2.534	8.914e-04	38.28
01/01/94	1925	-1.331e-04	2.701	0.000e-00	40.00
01/01/95	2290	-1.305e-04	2.695	0.000e-00	40.00

NOAA-14 Channel 1.

Date	Day post launch	a	b	c	d
30/12/94	0	0.000e-04	1.795	0.000e-04	41.0
01/01/95	2	-3.527e-04	1.795	0.000e-04	41.0
01/01/96	367	-3.047e-04	1.778	0.000e-04	41.0

[1] Source: Cihlar and Teillet, 1995 for NOAA-11 and Rao (NOAA/NESDIS) for NOAA-14

NOAA-14 Channel 2.

Date	Day post launch	a	b	c	d
30/12/94	0	0.000e-04	2.364	0.000e-04	41.0
01/01/95	2	-6.161e-04	2.364	0.000e-04	41.0
01/01/96	367	-5.088e-04	2.324	0.000e-04	41.0

Dates of Launch of NOAA Satellites

NOAA 11	NOAA 14
September 24, 1988	December 30, 1994

8. APPENDIX B: WIND SPEED AT Z = 5M

Calculation of wind speed at z = 5m is following the main equation:

$$U_5 = \frac{U_{*eff}}{0.41} \times \ln\left(\frac{5}{z_{0m}}\right) \qquad (m/s)$$

With:

U_5	being the z = 5m wind velocity	*(m/s)*
U_{*eff}	the effective friction velocity	*(m/s)*
ln	the Natural Logarithm	*(-)*
z_{0m}	the aero-dynamical roughness length for momentum transport	*(m)*

- Calculation of z_{0m}

In the area of interest, being the irrigated Indus Basin, identify the maximum NDVI values. Once located, the crop type and stage should be determined to give the height of the crop. In this regard, agronomists and field survey officers have been very helpful, saving huge time and workload to get secondary data. The height of the max NDVI crop is related to the z_{0m} by the following relationship:

$h_v = 7 \times z_{0m}$ for crop vegetation *(m)*

Having the z_{0m} of the vegetation responding to the max NDVI, and assuming constant the Z_{0m} and NDVI values of the desert from the following table:

Land Cover	NDVI	Z0m
Vegetation	$NDVI_{max}$	$\frac{h_v}{7}$
Desert	0.02	0.002

And the relating equation between NDVI and Z_{0m}, $Ln(z_{0m}) = a + (b \times NDVI)$, Ln being Neperian Logarithm.

Therefore two equations can be drawn out for each land cover type, enabling to solve the two parameters *a* and *b*:

Crop vegetation $$Ln\left(\frac{h_v}{7}\right) = a + (b \times NDVI_{max})$$

Desert $$Ln(0.002) = a + (b \times 0.02)$$

As being:

$$b = \frac{(NDVI_{max} - 0.02)}{\left[Ln\left(\frac{h_v}{7}\right) - Ln(0.002)\right]} \quad \text{and} \quad a = Ln(0.002) - [b \times (0.02)]$$

Finally, the Raster image of z_{0m} can be processed based on the NDVI one, following the equation below:

$$z_{0m} = EXP(a + b \times NDVI) \qquad (m)$$

- <u>Calculation of U_{*eff}</u>

$$U_{*eff} = 1282.1 \times \left(\frac{\partial r_0}{\partial T_0}\right)^2 + 47.821 \times \left(\frac{\partial r_0}{\partial T_0}\right) + 0.45 \qquad (m/s)$$

The parameter $\left(\frac{\partial r_0}{\partial T_0}\right)$ is calculated from the polynomial trend fitting regressive curve as an example given below:

R0	T0
2.21E-05	320.2234
0.118415	285.3986
0.12373	286.2597
0.127902	283.1543
0.128046	286.8671
0.134287	287.491
0.141812	288.1133
0.147944	288.723
0.156182	289.3445
0.170649	303.0762
0.172914	289.9771
0.176976	292.4892
0.177581	291.8675
0.180542	291.2315
0.18329	293.1129
0.184159	290.5941
0.189582	301.8152
0.196618	293.7412
0.205082	294.3687
0.209486	301.1869
0.215483	294.9985
0.218484	295.6287
0.221414	300.5665
0.223224	299.9449
0.225689	296.2511
0.230178	299.3338
0.231055	296.864
0.231864	298.108
0.231928	298.7257
0.232368	297.4801
0.25	296.5863
0.3	279.968

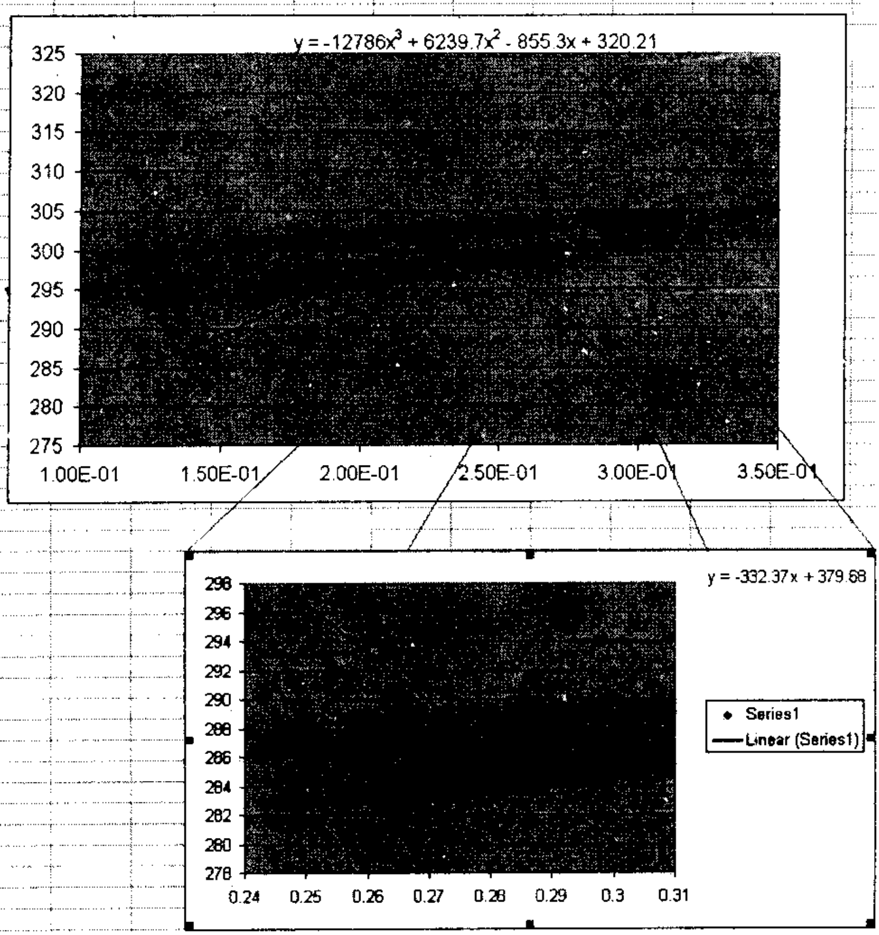

Figure 3 U_{*eff} calculation.

In this case for November 18th, 1993: $\left(\frac{\partial r_0}{\partial T_0}\right) = \frac{-1}{|Gain|} = \frac{-1}{|-332.37|} = 0.3181$

The method used to express r_0 in function of T_0 has different components, first is to get the T_0 image corrected upward onto sea level from height variations:

$T_0\_dem = T_0 + \left(\frac{0.6}{100}\right) \times DEM$	*(K)*

Second, is to follow this procedure in Erdas/Imagine:

1. Layer Stack the ρ_0 and *T_0_dem* images
2. Unsupervised classification with 30 classes
3. Signature editor, View/Columns/stats/means for each layer
4. Copy the two "means" columns and paste them in a spreadsheet

In the Spreadsheet, sort the columns on ρ_0 (called r_0 in Figure 3) in increasing order and draw a chart out of them, fit a polynomial (power 3) and reach Figure 3.

Practically, U_{*eff} is bounded from 0.1 to 0.45, any values out of these should be taken as their closest limit value.

9. FURTHER READINGS

Bastiaanssen W.G.M., 1998a. "Remote sensing in water resources management: the state of the art". International Water Management Institute (IWMI), Colombo, Sri Lanka: 118 pp.

Bastiaanssen W.G.M., Menenti M., Feddes R.A. and Holtslag A.A.M., 1998b. "A remote sensing surface energy balance algorithm for land (SEBAL), 1. Formulation". J. of Hydr. 212-213: 198-212

Bastiaanssen W.G.M., Thiruvengadarachi S., Sakhtivadivel R. and Molden D.J., 1999. "Satellite Remote Sensing For Estimating productivities of Land and Water". J. of Water Resources Development, Vol 15, Nos. 1/2, 181-196.

Bastiaanssen W.G.M., Chemin Y., Ahmad M.D., and Asif S., 1999. " Patterns of crop evaporation in the Indus Basin recognized from NOAA-AVHRR satellite " 17th ICID conference, Lausanne, Switzerland, 9p.

Brutsaert W. and Sugita M., 1992. "Application of self-preservation in the diurnal evolution of the surface energy budget to determine daily evaporation". J. of Geophysical Res., 97, D17: 18,322-18,377

Cooper D.I. and Asrar G., 1990. "Evaluating atmospheric correction models for retrieving surface temperatures from the AVHRR over a tall grass prairie". Remote Sensing of Environment, 27, 93-102.

Gordon C. and Erasmus J.F., 1995. "Automatic registration of NOAA AVHRR satellite Images". Institute of Soil, Climate and Water, Pretoria, South Africa.

Kaufman Y.J. and Holben B.N., 1993. "Calibration of the AVHRR visible and near-ir bands by atmospheric scattering, ocean glint and desert reflection". International Journal of Remote Sensing, 14, 21-52.

Kerdiles H., 1995 (?). "Software processing AVHRR data for the communities of Europe (SPACE): algorithms used in SPACE version 2. Part 1: Calibration, atmospheric correction and cloud detection". MARS project, TP 441, JRC – Space Applications Institute.

Rao C.R.N., 1993. "Non-linearity corrections for the thermal infrared channels of the Advanced Very High Resolution Radiometer: assessment and recommendations". NOAA Technical Report NESDIS-69, NOAA/NESDIS, Washington, DC.

Weinreb M.P., Hamilton G., Brown S. and Koczor R.J., 1990. "Nonlinearity corrections in calibration of Advanced Very high Resolution Radiometer infrared channels". Journal of Geophysics Research, 95, 7381-7388.